Journal of Alloys and Compounds 730 (2018) 483–486

Contents lists available at ScienceDirect

Journal of Alloys and Compounds

journal homepage: http://www.elsevier.com/locate/jalcom

Lorentz force induced magnetoelectric effect in cylindrical composites with PZT/magnetostrictive and nonmagnetic metal layers

Lirong Xu [a], Lijie Qiao [a], De'an Pan [b, *], Alex A. Volinsky [c]

[a] Corrosion and Protection Center, Key Laboratory for Environmental Fracture (MOE), University of Science and Technology Beijing, Beijing, 100083, PR China
[b] Institute of Circular Economy, Beijing University of Technology, Beijing, 100124, PR China
[c] Department of Mechanical Engineering, University of South Florida, Tampa, FL, 33620, USA

ARTICLE INFO

Article history:
Received 9 July 2017
Received in revised form
19 September 2017
Accepted 20 September 2017
Available online 21 September 2017

Keywords:
Magnetoelectric
Cylindrical composite
Lorentz force
Piezomagnetic

ABSTRACT

Lorentz force-piezoelectric coupled magnetoelectric (ME) effect and piezomagnetic-piezoelectric coupled ME effect were compared in PZT/nonmagnetic and PZT/magnetostrictive metal cylindrical layered composites under axial magnetic fields. While only the Lorentz force-piezoelectric ME effect is observed in PZT/brass and PZT/Al cylinders, both ME effects are present in PZT/magnetostrictive Ni cylinder. The ME voltage linear dependence on DC magnetic field and constant −90° ME voltage phase reflect the Lorentz force-piezoelectric ME effect. For the PZT/Ni cylinder under low DC magnetic field, the ME voltages from the two ME effects tend to be anti-phase, and the piezomagnetic-piezoelectric ME voltage is much higher than the Lorentz force-piezoelectric ME voltage. However, under high DC magnetic field, the Lorentz force-piezoelectric ME effect plays a dominant role. These results indicate that the PZT/Ni cylinder is favorable to DC magnetic field detection in wide range.

1. Introduction

Magnetoelectric (ME) effect is the coupling of magnetic and electric polarizations. In magnetostrictive and piezoelectric composites, the ME effect is a product of piezomagnetism and piezoelectricity via strain at the interface between the two phases [1–4]. At room temperature, multi-phase ME composites exhibit ME coupling coefficients several orders of magnitude higher than single-phase ME materials, especially for layered composites. This is promising in magnetic sensor, energy harvester, and other applications.

For the piezomagnetic-piezoelectric ME coupling, the ME voltage is proportional to the product of the piezoelectric voltage coefficient and the piezomagnetic coefficient ($q = d\lambda/dH$, where λ is line magnetostriction). The magnetoelectric voltage coefficient and q dependence on DC magnetic field (H_{DC}) is similar. For magnetostrictive and piezoelectric layered composites, the ME voltage increases first and subsequently decreases with H_{DC} to almost zero at high magnetic field beyond saturation. The local ME voltage peak appears at the optimal DC magnetic field, where the piezomagnetic coefficient reaches the maximum value [5–8]. However, for a cylindrical layered composite under magnetic field applied parallel to the cylinder axis, the ME voltage shows steep linear increase at high magnetic field after the peak, and is comparable or even higher than the ME voltage peak at optimal DC magnetic field. Pan et al. [9,10] ascribed this fact to linear volume magnetostriction of the self-bound Ni ring above saturation. However, the volume magnetostriction under high magnetic field is much smaller than the line magnetostriction, and the volume magnetostriction of polycrystalline nickel goes up with constant slope of 10^{-10} to 10^{-11} Oe^{-1} under increasing field [11–13], while the line magnetostriction slope at optimal DC magnetic field is about 10^{-7} Oe^{-1} [14]. Therefore, volume magnetostriction is unlikely to contribute significantly to linear ME voltage under high magnetic field.

Fetisov et al. [15] pointed out this linear dependence resulting from the piezoinductive effect through experimental and theoretical studies of a radially polarized piezoelectric ring with nonmagnetic conductive electrodes on the inner and outer surfaces. Conductive metal ring electrodes generated an electromotive force and then an AC current when AC magnetic field (H_{AC}) was applied perpendicular to the cylinder plane, according to the Faraday's law. The AC current carrying metal ring was subjected to uniform radial Ampere force when H_{DC} was applied parallel with

* Corresponding author.
E-mail address: pandean@bjut.edu.cn (D. Pan).

https://doi.org/10.1016/j.jallcom.2017.09.211
0925-8388/

the H_{AC}. Through interfacial mechanical coupling, the force was transferred to the piezoelectric ring creating tangential stress and outputing AC voltage due to piezoelectricity. The AC voltage u is:

$$u = \mu_0^2 \frac{g_{31}}{\rho} 2\pi r^2 t f H_{AC} H_{DC} \quad (1)$$

where μ_0 is the vacuum permeability, g_{31} is the piezoelectric voltage coefficient, r is the mean radius of the cylinder, t is the electrode thickness, and f is the frequency of the applied H_{AC}. The AC voltage is proportional to H_{DC}. Actually, the Ampere force is the result of the Lorentz forces of all moving charges, of which the current is comprised [16,17]. Therefore, the ME effect originates from the coupling of the Lorentz force and piezoelectricity in the piezoelectric ring with nonmagnetic conductive electrodes under axial magnetic field.

The thickness of the metal ring in the cylindrical layered composite from Ref. [15] is just several microns, which is greatly different from the 1 mm thickness of the Ni ring in the PZT/Ni cylindrical layered composite in Ref. [9]. Thus, the Lorentz force-piezoelectric coupled ME effect and the piezomagnetic-piezoelectric coupled ME effect cannot be directly compared. In all reports following the idea of the Lorentz force-piezoelectric coupled ME effect, an input reference AC current in the electrode is utilized to introduce the Lorentz force [18–21]. However, input AC current raises energy costs and induces electromagnetic interference. In this paper, we directly compare the two kinds of ME effects by characterizing the ME voltage outputs and the corresponding phases of the PZT/nonmagnetic and PZT/magnetostrictive metal cylindrical layered composites with the same dimensions in the axial mode.

2. Experiment

Three different PZT and metal cylindrical layered composites were prepared, as illustrated in Fig. 1. Three PZT-5H ceramic rings with $\Phi 25 \times \Phi 23 \times 10$ mm^3 dimensions were radially polarized at the same time. Nonmagnetic brass and aluminum rings were separately bonded on the inner surfaces of two PZT rings with conductive silver adhesive, while magnetostrictive nickel was directly electrodeposited on the inner surface of the third PZT ring to avoid the influence of nonmagnetic silver layer. The metal rings are all about 300 μm thick. Nickel electrodeposition is described elsewhere [9]. The three cylinders are named PZT/brass, PZT/Al and PZT/Ni. The ME characterization was performed in the ME measurement system with both DC (H_{DC}) and AC (H_{AC}) magnetic fields applied parallel to the cylinder axis (axial mode). The ME voltage coefficient, $\alpha_{E,A}$, was calculated as $\alpha_{E,A} = \delta V/(t_{PZT} \cdot \delta H)$, where δV is the amplitude of the ME voltage in the PZT ring, t_{PZT} is the PZT ring thickness and δH is the amplitude of the applied AC magnetic field. The ME voltage phase, φ, between the ME voltage and H_{AC} was measured simultaneously.

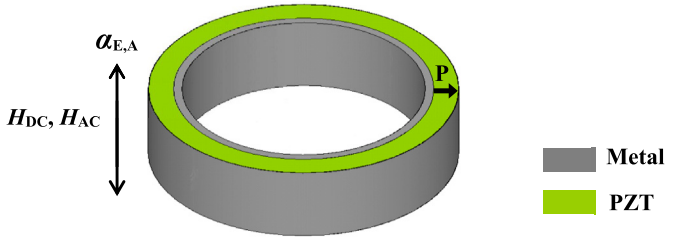

Fig. 1. Illustration of the PZT and metal cylindrical layered ME composite.

3. Results and discussion

Fig. 2 shows the axial ME voltage coefficient, $\alpha_{E,A}$, and the phase, φ, dependence on the AC magnetic field frequency, f, for the three cylinders under the optimal DC magnetic field ($H_{DC} = 230$ Oe) of the PZT/Ni cylindrical layered composite. For the PZT/Ni cylinder, there are two ME resonance peaks. The ME resonance corresponds to the electromechanical anti-resonance frequency (f_a) of the piezoelectric layer [22] and the first one corresponds to the fundamental radial extension vibration mode while the second one happens at second radial extension vibration mode [23]. A phase shift of about 180° happens at the first peak, and the phase shifts by approximately 140° at the second peak. This means that the ME resonance quality is reduced at higher resonance mode. By contrast, PZT/brass and PZT/Al nonmagnetic metal cylindrical layered composites have almost invisible ME resonance peaks, as seen in Fig. 2. Both corresponding phases around the fundamental extensional mode change by about 180°. With expanded $\alpha_{E,A}$ scale, the ME resonance peaks of the PZT/brass and PZT/Al cylinders can be seen in the inset in Fig. 2. The PZT/brass cylinder's peak is higher than that of the PZT/Al cylinder, but the peak value of 0.068 V/cm Oe is two orders of magnitude lower than the PZT/Ni cylinder's. Moreover, the PZT/Ni cylinder has much higher ME voltage in entire frequency range under low H_{DC}. Obviously, the voltage outputs in the two PZT/nonmagnetic metal cylinders can only come from the Lorentz force-piezoelectric ME effect though their peaks are rather small at low H_{DC}, and that of the PZT/Ni cylinder is generated from the piezomagnetic-piezoelectric ME effect.

For PZT/Ni, PZT/Al and PZT/brass cylinders at high DC magnetic field ($H_{DC} = 2$ kOe), the frequency dependence of $\alpha_{E,A}$ is shown in Fig. 3. The first ME resonance peaks corresponding to the fundamental radial extension modes of the three cylinders are comparable with each other, as well as in off-resonant frequency range. At high H_{DC}, the two PZT/nonmagnetic metal cylinders' peaks are enhanced by an order of magnitude, while the PZT/Ni cylinder's peak is reduced. The trend is the same for the three cylinders in the entire frequency range. In addition, the second weak ME resonance peaks appear in the two PZT/nonmagnetic metal cylinders, which are unobservable under low H_{DC} in inset of Fig. 2 as the $\alpha_{E,A}$ scale

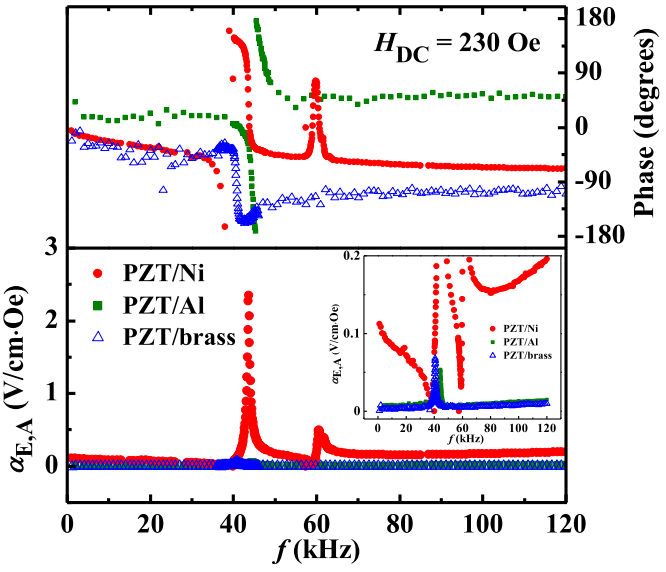

Fig. 2. AC magnetic field frequency dependence of the ME voltage coefficient $\alpha_{E,A}$ and the corresponding phase φ of the PZT/Ni, PZT/Al and PZT/brass cylinders under the PZT/Ni cylinder optimal DC magnetic field. The inset shows enlarged $\alpha_{E,A}$ scale.

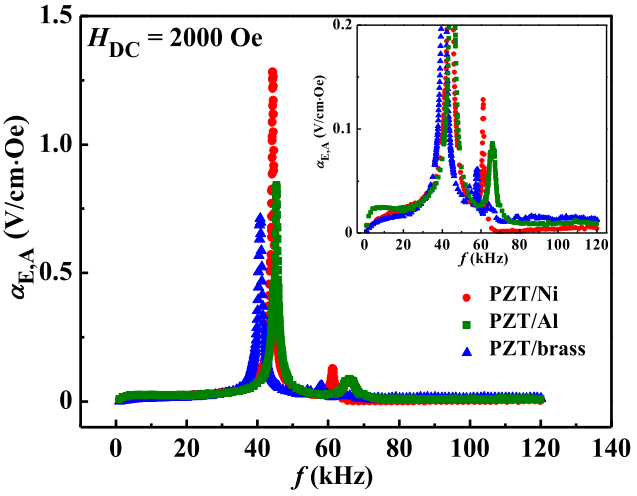

Fig. 3. Frequency dependence of the ME voltage coefficient $\alpha_{E,A}$ for three cylinders under high DC magnetic field H_{DC} = 2 kOe. The inset shows enlarged $\alpha_{E,A}$ scale.

was refined. Considering that the ME effect of the PZT/Al and PZT/brass cylinders originate from the coupling of the Lorentz force and the piezoelectric effect, similar ME voltage output of the PZT/Ni cylinder at high H_{DC} may also be the result of the same ME coupling.

Fig. 4 shows the DC magnetic field dependence of the ME voltage coefficient $\alpha_{E,A}$ for the PZT/Ni, PZT/Al and PZT/brass cylinders at off-resonant frequency f = 1 kHz. In the entire DC magnetic field range, the ME voltage outputs are rather small for all the three cylinders, which coincides with the results present in Figs. 2 and 3. Inevitably, the measured ME voltage is greatly influenced by the background noise [24] and the data in Fig. 4 fluctuate. Nevertheless, different variation trends of $\alpha_{E,A}$ with H_{DC} are observed in the PZT/nonmagnetic and PZT/magnetostrictive cylinders. In the PZT/Ni cylinder, as H_{DC} is increased from zero, $\alpha_{E,A}$ increases rapidly to the maximum and then decreased to the minimum, which is typical for magnetostrictive and piezoelectric layered composites. Strengthening H_{DC} further, a gentle enhancement in $\alpha_{E,A}$ appears. For the PZT/Al and PZT/brass cylinders in entire H_{DC} range, gentle trends of $\alpha_{E,A}$ increase with H_{DC} are also present. The increase trends agree with the prediction in equation (1). It is worth noting that the ME voltage in the PZT/Ni cylinder is much higher than those in the PZT/Al and PZT/brass cylinders under low H_{DC} but lower under high H_{DC}.

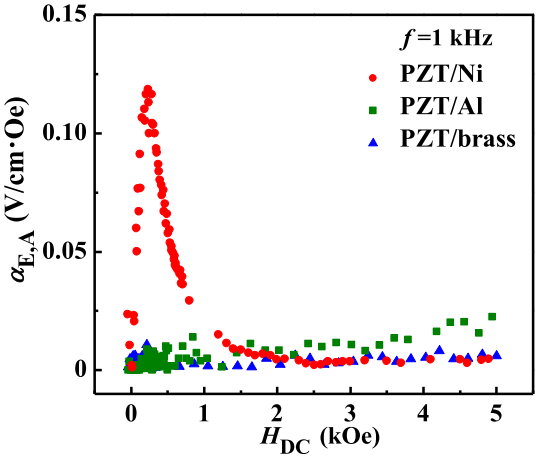

Fig. 4. Dependence of the ME voltage coefficient $\alpha_{E,A}$ on DC magnetic field for the PZT/Ni, PZT/Al and PZT/brass cylinders at frequency f = 1 kHz.

It further confirms that the ME voltage in the PZT/Ni cylinder under low H_{DC} is mainly due to the piezomagnetic-piezoelectric ME effect.

Fig. 5 shows $\alpha_{E,A}$ and φ dependence on H_{DC} for the PZT/brass, PZT/Al and PZT/Ni cylinders at each fundamental radial extension resonant frequency in axial mode. Unlike off-resonance range in Fig. 4, the three cylinders each has great ME voltage output. The curves are scarcely affected by the background noise. The two PZT/nonmagnetic metal cylinders have linear H_{DC} dependence of the $\alpha_{E,A}$ over the whole DC magnetic field range, since both fits show good linearity ($R^2 \geq 0.997$). This is consistent with equation (1). The y axis intercepts of the fitting lines are −0.015 V/cm Oe and −0.012 V/cm Oe for the PZT/Al and PZT/brass cylinders, respectively. Small negative intercept values are due to the fact that the measured curves shift to the right, since H_{DC} recorded by the Hall sensor is larger than the effective magnetic field in cylinders, owing to the opposite magnetic field caused by self-inductance in the metal ring. Nevertheless, these results verify that the ME voltage output in PZT/non-magnetic metal cylinder comes from the Lorentz force-piezoelectric ME effect.

Under low H_{DC}, the PZT/Ni cylinder's $\alpha_{E,A}$ increases with H_{DC} to the local maximum value of 2.44 V/cm Oe and then decreases with H_{DC}, similar to the tendency at off-resonant frequency far from resonance in Fig. 4. The $\alpha_{E,A}$ of the PZT/Ni cylinder is much higher than the two PZT/non-magnetic metal cylinders, until the $\alpha_{E,A}$ is reduced to the local minimum value of 0.365 V/cm·Oe at H_{DC} = 0.9 kOe. The minimum value of the PZT/Ni cylinder is still slightly higher. The above observations indicate that the ME effect is mainly due to the piezomagnetic-piezoelectric coupling in the PZT/Ni cylinder under low H_{DC}. Starting from H_{DC} = 0.9 kOe, the $\alpha_{E,A}$ of the PZT/Ni cylinder increases linearly with H_{DC}. The $\alpha_{E,A}$ is quite larger for the electrodeposited PZT/Ni cylinder. The fitting lines show good linearity ($R^2 \geq 0.997$) for all cylinders. The large slope linear region can be used for high DC magnetic field detection. On the other hand, as the total ME voltage output in low DC magnetic field is comparable to that in high DC magnetic field in the PZT/Ni cylinder, the magnetic field detectivity won't be reduced within wide range.

As shown in Fig. 5, the $\varphi = -80°$, of the PZT/Ni cylinder does not change under high H_{DC}. In both PZT/nonmagnetic metal cylinders, φ

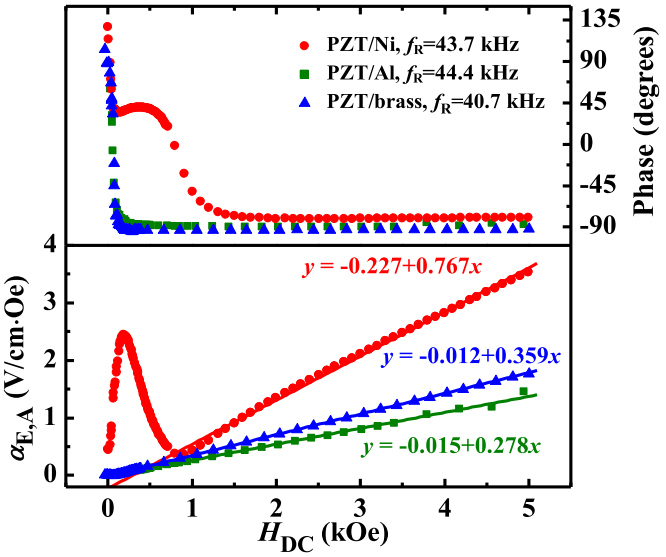

Fig. 5. DC magnetic field dependence of the ME voltage coefficient $\alpha_{E,A}$ and the corresponding phase φ for the PZT/Ni, PZT/Al and PZT/brass cylinders at each radial extension resonant frequency.

is almost −93° immediately after H_{DC} cross zero. In the Lorentz force-piezoelectric ME effect, assuming the AC magnetic field is $H_{AC} = h \sin \omega t$, the induced electromotive force in the metal ring is

$$e = -\frac{d(S\mu_0 h \sin \omega t)}{dt} = -\mu_0 hS \cos \omega t = \mu_0 hS \sin(\omega t - 90^\circ) \quad (2)$$

where h is the amplitude of the H_{AC}, ω is the annular frequency of H_{AC}, and S is the circle area of the ring. Irrespective of the inductance of the metal ring, the AC current lags 90° behind H_{AC}, i.e. the φ of the AC current is −90°. Leung et al. demonstrated that the ME voltage from the piezoelectric layer is in phase with the AC current in the electrode [25]. On the other hand, the impedance phase of the anti-electromechanical resonance is zero. Therefore, the φ is −90° for the two PZT/nonmagnetic metal cylinders at ME resonance. In this experiment, the φ is slightly off −90° as a result of the electrode inductance, experimental and real resonant frequency errors and slight differences among the three cylinders. For the PZT/Ni cylinder, φ is rapidly reduced to 34.6° at H_{DC} crossing zero, where the $\alpha_{E,A}$ reaches local maximum. At higher H_{DC}, φ increases to 40° and then gradually decreases to −80° in the PZT/Ni cylinder. In the piezomagnetic-piezoelectric ME effect, the magnetic loss changes with H_{DC} due to the irreversible magnetic domain motion and rotation. Moreover, the ME resonant frequency changes with increasing H_{DC}, which is caused by the ΔE effect in the magnetostrictive layer, so the phase of the piezomagnetic-piezoelectric ME effect is strongly dependent on H_{DC} [26]. The φ of −80° under high H_{DC} is further proof of the dominant Lorentz force-piezoelectric ME effect in the PZT/Ni cylinder.

It has been known that both ME effects contribute to the ME voltage in the PZT/Ni cylinder. The correlation between the two ME effects is discussed below. The y axis intercept of the fitting line for the PZT/Ni cylinder under high H_{DC} is −0.227 V/cm Oe, which is more negative than the two PZT/nonmagnetic metal cylinders. If ME voltages from the two ME effects add up, the intercept should be higher than those of the other two cylinders. However, the ME voltage is a complex quantity, thus, the ME phase needs to be considered. The more negative intercept may result from the cancellation of the two ME effects with opposite phases. In the case of the point when the $\alpha_{E,A}$ reaches the local maximum, $\varphi = 34.6^\circ$. Based on the parallelogram law of complex superposition, the phase of the piezomagnetic-piezoelectric ME effect must be larger than 34.6°, so the phase difference of two ME effects is more than 120°. This inclines to anti-phase and the total ME voltage of the PZT/Ni cylinder is less than either one of the two ME effects. Below the H_{DC} where the minimum $\alpha_{E,A}$ happens with $\varphi = 0^\circ$, the phase of the piezomagnetic-piezoelectric ME effect should also be positive. Beyond saturation, nickel is paramagnetic, similar to non-magnetic brass and aluminum. Thus, the voltage originating from the piezomagnetic-piezoelectric ME effect tends toward zero. Both the ME phase and voltage of the PZT/Ni cylinder are mainly based on the Lorentz force-piezoelectric ME effect at high H_{DC}. On the other hand, the linear region at high H_{DC} indicates that the piezomagnetic-piezoelectric ME effect is also linear with H_{DC}, which in turn reflects nickel linear volume magnetostriction.

4. Conclusion

Both linear H_{DC} dependence of the $\alpha_{E,A}$ and φ of approximately −90° demonstrated the Lorentz force-piezoelectric coupled ME effect for PZT/metal cylindrical layered composites with magnetic fields applied parallel to the cylinder's axis. In the axial mode, both the piezomagnetic-piezoelectric ME and Lorentz force-piezoelectric ME effects contribute to ME voltage output in the PZT/Ni cylinder. For the PZT/Ni cylinder under low DC magnetic field, the ME voltage from the Lorentz force-piezoelectric ME effect is much lower than the piezomagnetic-piezoelectric ME effect. Under high DC magnetic field, the piezomagnetic-piezoelectric ME effect is close to zero, so the linear ME voltage is primarily due to the Lorentz force-piezoelectric ME effect. The high ME voltage output in low DC magnetic field and large slope linear region in the PZT/Ni cylinder can be utilized for DC magnetic field detection in wide range.

Acknowledgements

This work was supported by the Beijing Nova Program, China (Z141103001814006), the Fundamental Research Funds for the Central Universities (Project No: FRF-TP-14-001C1) and the National Science Foundation (IRES 1358088).

References

[1] W. Eerenstein, N.D. Mathur, J.F. Scott, Nature 442 (2006) 759–765.
[2] G. Srinivasan, Annu. Rev. Mater. Res. 40 (2010) 153–178.
[3] J.M. Hu, L.Q. Chen, C.W. Nan, Adv. Mater. 28 (2016) 15–39.
[4] Y. Jia, H. Luo, X. Zhao, F. Wang, Adv. Mater. 20 (2008) 4776–4779.
[5] G.L. Yu, H.W. Zhang, Y.X. Li, J. Li, Compd. Struct. 108 (2014) 287–294.
[6] Y.K. Fetisov, D. Chashin, N.A. Ekonomov, D.A. Burdin, Y.F. Leonid, IEEE Trans. Magn. 51 (11) (2015) 2503403.
[7] N.O. Urs, I. Teliban, A. Piorra, R. Knöchel, E. Quandt, J. McCord, Appl. Phys. Lett. 105 (2014) 202406.
[8] Y. Zhou, D. Maurya, Y. Yan, G. Srinivasan, E. Quandt, S. Priya, Energy Harvest. Syst. 3 (1) (2016) 1–42.
[9] D.A. Pan, Y. Bai, A.A. Volinsky, W.Y. Chu, L.J. Qiao, Appl. Phys. Lett. 92 (2008), 052904.
[10] D.A. Pan, J. Wang, Z.J. Zuo, S.G. Zhang, L.J. Qiao, A.A. Volinsky, Appl. Phys. Lett. 105 (2014) 102902.
[11] É. du Trémolet de Lacheisserie, D. Gignoux, M. Schlenker, Magnetism, Springer New York, 2002, pp. 351–354.
[12] V.I. Nizhankovskii, Eur. Phys. J. B 53 (2006) 1–4.
[13] R.C. Hall, J. Appl. Phys. 30 (1959) 1459.
[14] H.E. Lee, D.T. Peters, G.D. Sandrock, IEEE Trans. Magn. 9 (4) (1973) 636–640.
[15] Y.K. Fetisov, D.V. Chashin, G. Srinivasan, J. Appl. Phys. 106 (044103) (2009).
[16] Y.M. Jia, D. Zhou, L.H. Luo, X.Y. Zhao, H.S. Luo, S.W. Or, H.L.W. Chan, Appl. Phys. A 89 (2007) 1025–1027.
[17] Y.M. Jia, Y.X. Tang, X.Y. Zhao, H.S. Luo, S.W. Or, H.L.W. Chan, J. Appl. Phys. 100 (2006) 126102.
[18] Y.K. Fetisov, IEEE Sens. J. 14 (6) (2014) 1817–1821.
[19] I.M. Krykanov, A.B. Koplik, Y.K. Fetisov, D.V. Chashin, Tech. Phys. Lett. 36 (9) (2010) 838–840.
[20] L. Zhang, S.W. Or, C.M. Leung, S.L. Ho, J. Appl. Phys. 115 (2014) 17E520.
[21] L. Zhang, S.W. Or, C.M. Leung, J. Appl. Phys. 117 (2015) 17A748.
[22] L.R. Xu, D.A. Pan, L.J. Qiao, A.A. Volinsky, Y. Song, Mater. Des. 89 (2016) 173–176.
[23] Z. Wu, Z. Xiang, Y. Jia, Y. Zhang, H. Luo, J. Appl. Phys. 112 (2012) 106102.
[24] Y.J. Wang, J.Q. Gao, M.H. Li, Y. Shen, D. Hasanyan, J.F. Li, D. Viehland, Philos. Trans. R. Soc. A 372 (2014), 20120455.
[25] C.M. Leung, S.W. Or, S.L. Ho, J. Appl. Phys. 107 (2010), 09E702.
[26] Z. Shi, L. Chen, Y. Tong, H. Xue, S. Yang, C. Wang, X. Liu, Appl. Phys. Lett. 102 (2013) 112904.